Journal of Organometallic Chemistry, 329 (1987) 85–97
Elsevier Sequoia S.A., Lausanne – Printed in The Netherlands

1,3-Diaryltriazenido complexes of bis-cyclopentadienylmolybdenum. Preparation and electrochemical behaviour

M.A.M. Queirós, J.E.J. Simão

Centro de Química Pura e Aplicada, Universidade do Minho, 4719 Braga Codex (Portugal)

and A.R. Dias

Centro de Química Estrutural, Complexo I, Instituto Superior Técnico, 1096 Lisboa Codex (Portugal)

(Received December 9th, 1986)

Abstract

The new complexes $[Mo(\eta\text{-}C_5H_5)_2(p\text{-}R^1C_6H_4NNN\text{-}p\text{-}C_6H_4R^2)][PF_6]$ (**1**) ($R^1 = R^2 = H, F, CH_3, OCH_3$; $R^1 = H$, $R^2 = CH_3, OCH_3$; $R^1 = CH_3$, $R^2 = OCH_3$) have been prepared. The electrochemical behaviour of these complexes in acetonitrile has been studied by cyclic voltammetry and constant potential electrolysis at platinum electrodes. The complexes undergo two reversible one-electron reductions to species which are stable on the cyclic voltammetry time scale, but the uptake of electrons appears to be followed by loss of the triazenido ligand. The oxidative electrochemistry of the complexes can be rationalized in terms of a disproportionation occurring after the first one-electron oxidation. Both reduction and oxidation potentials show good linear correlations with σ^+ Hammett parameters, providing evidence for the mesomeric influence of ligand R^1 and R^2 substituents on the metal orbitals involved in the redox processes.

Introduction

Most of the work on complexes containing 1,3-diaryltriazenido ligands is centered on the syntheses, reactivities, and coordination modes of these ligands. X-ray diffraction studies show that they can be monodentate, chelate, or bridging, or undergo orthometallation [1]. There have been no previous reports of 1,3-diaryltriazenido complexes containing the $Mo(\eta^5\text{-}C_5H_5)_2$ moiety.

In recent years there has been increased interest in the electrochemistry of metal complexes [2], but little attention has been paid to the redox chemistry of 1,3-diaryltriazenido complexes [3]. In this paper we describe the synthesis and characteri-

0022-328X/87/$03.50

Table 1

Analytical, conductimetric and ^{1}H NMR data

Complex	Analysis (Found (calc) (%))			M.p. (°C)	Λ [a] (Ω^{-1} cm^2 mol^{-1})	^{1}H NMR spectra [b] τ (multiplicity; intensity)				
	C	H	N			CH$_3$	OCH$_3$	C$_5$H$_5$	Ar	
[MoCp$_2$(dat)][PF$_6$] (**1a**)	45.31 (45.95)	4.04 (3.86)	6.12 (6.70)	265	80	–	6.18(s,6)	3.82(s,10)	3.03(s,4) 3.05(s,4)	
[MoCp$_2$(att)][PF$_6$] (**1b**)	46.84 (47.15)	3.92 (3.96)	6.70 (6.87)	258	85	7.69(s,3)	6.20(s,3)	3.82(s,10)	2.86(d,2) 3.03(s,2)	3.05(s,3) 3.08(s,1)
[MoCp$_2$(apt)][PF$_6$] (**1c**)	46.04 (46.26)	3.92 (3.71)	6.99 (7.03)	272	82	–	6.22(s,3)	3.81(s,10)	2.70(d,2) 3.08(m,7)	
[MoCp$_2$(dtt)][PF$_6$] (**1d**)	48.55 (48.42)	3.85 (4.06)	6.99 (7.06)	270	88	7.68(s,6)	–	3.79(s,10)	2.85(s,1) 2.87(s,3)	3.05(s,1) 3.08(s,3)
[MoCp$_2$(ptt)][PF$_6$] (**1e**)	47.35 (47.52)	3.94 (3.81)	7.15 (7.23)	275	90	7.67(s,3)	–	3.77(s,10)	2.66(t,2) 2.81(t,1)	2.90(q,4) 3.03(d,2)
[MoCp$_2$(dfft)][PF$_6$] (**1f**)	43.06 (43.80)	3.01 (3.01)	6.37 (6.97)	280	95	–	–	3.74(s,10)	2.88(s,4) 2.90(s,4)	
[MoCp$_2$(dpt)][PF$_6$] (**1g**)	46.65 (46.41)	3.70 (3.55)	6.79 (7.41)	278	95	–	–	3.80(s,10)	2.75(m,6) 2.90(m,4)	

[a] In 10^{-3} *M* nitromethane solutions. [b] In Me$_2$CO-d_6 as solvent and TMS as internal reference.

zation of a series of complexes of the type $[\mathrm{Mo}(\eta\text{-}C_5H_5)_2(p\text{-}R^1C_6H_4NNN\text{-}p\text{-}C_6H_4R^2)][PF_6]$ (**1**) as well as the oxidative and reductive electrochemistry of these closed shell complexes. The dependence of the energy of the redox orbitals on the nature of the substituents is also considered.

Chemical studies

Compounds $[MoCp_2X_2]$ ($Cp = \eta^5\text{-}C_5H_5$; X = Cl, Br, I) react with 1,3-diaryltriazenes (triH) in refluxing ethanol in the presence of triethylamine to yield the monocations $[MoCp_2(tri)]^+$, which were isolated as hexafluorophosphate salts, **1**. These complexes were also prepared from either $[MoCp_2HI]$ or $[MoCp_2Hpy][PF_6]$ under the same conditions. Refluxing triH with either $[MoCp_2H_2]$ or $[MoCp_2H_3][PF_6]$ in ethanol in the absence of triethylamine also afforded complexes **1**, although in the latter case the yield was lower. The structure proposed below is consistent with the analytical and spectroscopic data presented in Table 1.

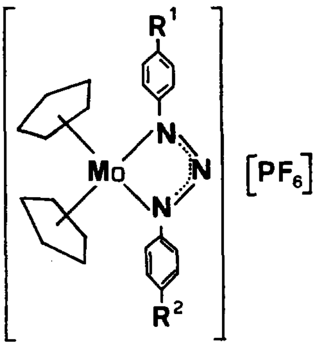

	R^1	R^2	
1a	OCH_3	OCH_3	dat
1b	CH_3	OCH_3	att
1c	H	OCH_3	apt
1d	CH_3	CH_3	dtt
1e	H	CH_3	ptt
1f	F	F	dfft
1g	H	H	dpt

The IR spectra show bands characteristic of the cyclopentadienyl rings (3120 cm^{-1}) and of the PF_6^- anion (840, 560 cm^{-1}), together with bands due to the 1,3-diaryltriazenido ligands at ca. 1600 and 1300 cm^{-1}. The ^1H NMR spectra, besides showing the peak due to the cyclopentadienyl rings (3.74–3.82 τ), also show peaks in the aromatic region due to the phenyl rings of the ligands and one peak (when $R^1 = R^2$) or two peaks (when $R^1 \neq R^2$) due to the substituents. The conductimetric data are consistent with previously reported values for 1 : 1 electrolytes [4]. Attempts to bring complexes **1** into reaction with PPh_3, C_5H_5N, CH_3CN, NH_3 and HCl always resulted in recovery of the starting complex.

All attempts to prepare the tungsten analogues of complexes **1** were unsuccessful.

Electrochemical studies

Cyclic voltammograms for all the complexes were recorded with solutions in acetonitrile (concentrations ca. 10^{-3} mol dm^{-3}) containing tetrabutylammonium hexafluorophosphate (10^{-1} mol dm^{-3}) at a Pt electrode. The cyclic voltammogram in Fig. 1 is typical for these complexes, and shows redox processes at the negative potentials (1,2), together with redox processes at the positive potentials (3, 4 and 5).

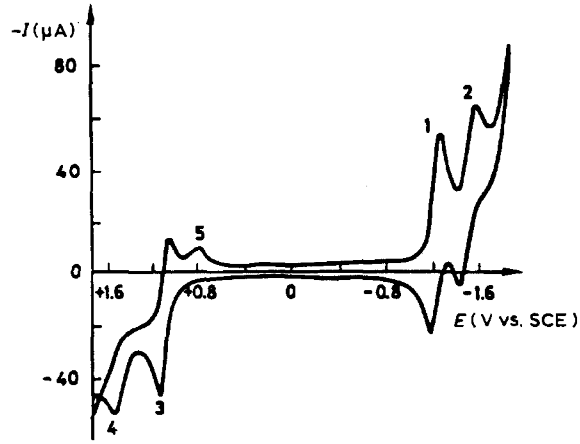

Fig. 1. Cyclic voltammogram of complex **1b** (1.30×10^{-3} mol dm^{-3}) in acetonitrile containing $[Bu_4N][PF_6]$. Pt electrode, potential scan rate; 0.10 V s^{-1}.

Reductive processes

Data from cyclic voltammograms at scan rates between 0.02 and 0.50 V s^{-1} are listed in Table 2a. Two reversible one-electron reduction processes are observed, the species obtained after each reduction being stable on the time scale of the experiments (1–80 s). The voltammograms for complex **1f** ($R^1 = R^2 = F$) show only one monoelectronic wave with a peak current ratio lower than one, suggesting that the species formed after reduction of this complex is less stable. The reason for this is not clear.

The current function, $^1I_p^c v^{-1/2} c^{-1}$, for each complex is constant over the range of scan rates used. From these values and those obtained for the pair $FeCp_2/FeCp_2{}^+$, under the same conditions, the diffusion coefficients were estimated (Table 2a).

These observations indicate that the reductions follow the scheme:

$$\underset{18\text{ e}}{[MoCp_2(tri)]^+} \underset{-e}{\overset{+e}{\rightleftarrows}} \underset{19\text{ e}}{[MoCp_2(tri)]} \underset{-e}{\overset{+e}{\rightleftarrows}} \underset{20\text{ e}}{[MoCp_2(tri)]^-}$$

It is of interest to compare the behaviour of these complexes with that of other complexes containing the MCp_2 fragment. Kotz et al. [5] observed two monoelectronic and irreversible reductions between −0.95 and −1.10 V for the complexes $[MCp_2X_2]$ (M = Mo, W; X = Cl, Br, I) in acetonitrile. For these complexes the 19 and 20 electrons species obtained after the first and second reductions are unstable, and lose the excess of negative charge by liberating X^- after cleavage of the M–X bond, with formation of $[MCp_2(NCMe)X]^-$. After reduction of the complexes $[MCp_2Cl_2]$ (M = Ti, V, Nb) [6] there is a fast loss of Cl^-, which is replaced by a neutral ligand (pyridine or solvent). This behaviour is dependent on the bonding ability of the solvent, as a pseudo-reversible wave is observed in THF owing to the return of the Cl^-.

The higher stability of the species obtained after reduction of our complexes (with exception of complex **1f**) must be related to the delocalisation of the negative charge over the chelated diaryltriazenido ligands. The stabilising effect of chelated

Table 2

Cyclovoltammetric data for complexes $[MoCp_2(tri)][PF_6]$ in acetonitrile containing $[Bu_4N][PF_6]$ (Pt electrode)

(a) Reduction

Complex	R^1	R^2	$-^1E_p^c$ (V) [a]	Δ^1E_p (mV) [b]	$^1I_p^a/^1I_p^c$	$-^1I_p^c v^{-1/2} c^{-1}$ [c] (A $V^{-1/2}$ $s^{1/2}$ cm^3 mol^{-1})	$-^2E_p^c$ (V) [a]	Δ^2E_p (mV) [b]	$^2I_p^a/^2I_p^c$	10^5D (cm^2 s^{-1})
$[MoCp_2(dat)][PF_6]$ (**1a**)	OCH_3	OCH_3	1.34	70	1.0	110	1.58	70	1.0	1.9
$[MoCp_2(att)][PF_6]$ (**1b**)	OCH_3	OCH_3	1.31	70	1.0	110	1.56	90	1.0	1.9
$[MoCp_2(apt)][PF_6]$ (**1c**)	OCH_3	H	1.27	70	1.0	115	1.52	90	1.0	2.0
$[MoCP_2(dtt)][PF_6]$ (**1d**)	CH_3	CH_3	1.29	70	1.0	110	1.59	90	1.0	1.9
$[MoCp_2(ptt)][PF_6]$ (**1e**)	CH_3	H	1.28	70	1.0	110	1.56	80	1.0	1.9
$[MoCp_2(dfft)][PF_6]$ (**1f**)	F	F	1.24	80	0.8	110	1.48	–	–	1.9
$[MoCp_2(dpt)][FP_6]$ (**1g**)	H	H	1.25	70	1.0	100	1.57	80	1.0	1.9

(b) Oxidation

Complex	R^1	R^2	$^3E_p^A$ (V)	ΔE (mV) [b]	$^3I_p^c/^3I_p^a$ [b]	$^3I_p^a v^{-1/2} c^{-1}$ [b,c] (A V^{-1} $s^{1/2}$ cm^3 mol^{-1})	$^4E_p^a$ (V) [a]	$^5E_p^c$ (V)	10^7K_D (298 K)	Lifetime (s)
$[MoCp_2(dat)][PF_6]$ (**1a**)	OCH_3	OCH_3	1.03	70	1.0	140	1.40	0.81	5.4	
$[MoCp_2(att)][PF_6]$ (**1b**)	OCH_3	CH_3	1.15	70	1.0	140	1.51	0.84	7.9	
$[MoCp_2(apt)][PF_6]$ (**1c**)	OCH_3	H	1.20	70	1.0	140	1.53	0.90	25.5	
$[MoCp_2(dtt)][PF_6]$ (**1d**)	CH_3	CH_3	1.29	70	1.0	130	1.60	–	3.6	
$[MoCp_2(ptt)][PF_6]$ (**1e**)	CH_3	H	1.35	90	0.6	150	–	1.15	–	0.8
$[MoCp_2(dfft)][PF_6]$ (**1f**)	F	F	1.38	70	0.8	140	–	–	–	6.1
$[MoCp_2(dpt)][PF_6]$ (**1g**)	H	H	1.42	90	0.5	160	–	1.18	–	0.006

[a] Potentials vs. SCE. [b] Values measured at 0.20 V s^{-1}. [c] The current function for the $FeCp_2/FeCp_2^+$ couple was 120 A $V^{-1/2}$ $s^{1/2}$ cm^3 mol^{-1}.

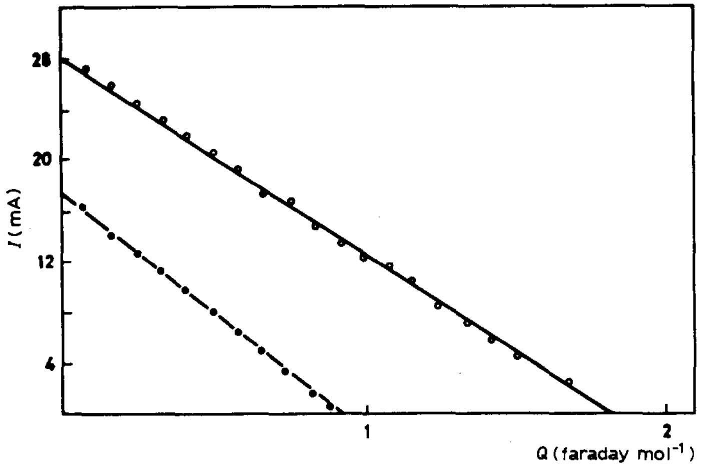

Fig. 2. Plots of charge passed vs. cell current for the electrolysis of 48 μmol of complex **1a** in acetonitrile containing $[Bu_4N][PF_6]$. Electrolysis at −1.36 V (●) and −1.62 V (○).

ligands possessing delocalised electron systems has been observed for other complexes [7–9].

Constant potential electrolyses at a potential of ca. 40 mV cathodic to the first wave were carried out. For all complexes the current, monitored against the charge passed, decays after the passage of 0.98–0.99 F mol^{-1} to a background level (Fig. 2). The catholyte changes in colour from red to brownish-yellow. Both cathodic and its coupled anodic peaks decrease in intensity during electrolysis until complete disappearance, showing that the 19-electron species formed are unstable on the time scale of the experiment (30 min). New redox processes are observed, one appearing at a potential at which the free diaryltriazenido ligand is oxidised. This suggests that there is displacement of this ligand after the uptake of one electron. The electrolyses carried out at potentials after the second peak show the consumption of 1.80 to 1.84 F mol^{-1} (Fig. 2) and the catholyte changes from red to yellow. After these electrolyses both reduction waves disappear, there is again evidence for the liberation of the diaryltriazenido ligand from all the complexes.

Oxidative processes

Complexes **1a**, **1b** and **1c** show two one-electron oxidation processes (3,4) at the positive potentials together with a reduction wave (5) at less positive potentials. For these complexes the first redox process is electrochemically reversible at scan rates higher that 0.10 V s^{-1} if the scan is reversed before the second peak (Fig. 3a). This peak has the characteristics of an EC process for which the chemical reaction is very fast, since no cathodic counterpart is observed at scan rates up to 50 V s^{-1} (lifetime 10^{-3} s). Peak 5 is always observed when the scan is reversed after the second wave. The electrochemical data are listed in Table 2b.

When the potential is held for several seconds at a potential close to $^{3}E_p^a$ before the scan is reversed, the current ratio diminishes and peak 5 is also observed (Fig. 3b). This shows that the dication formed after the one-electron oxidation undergoes a chemical reaction, and reveals that the species responsable for wave 5 is also formed by a slow reaction of the dication.

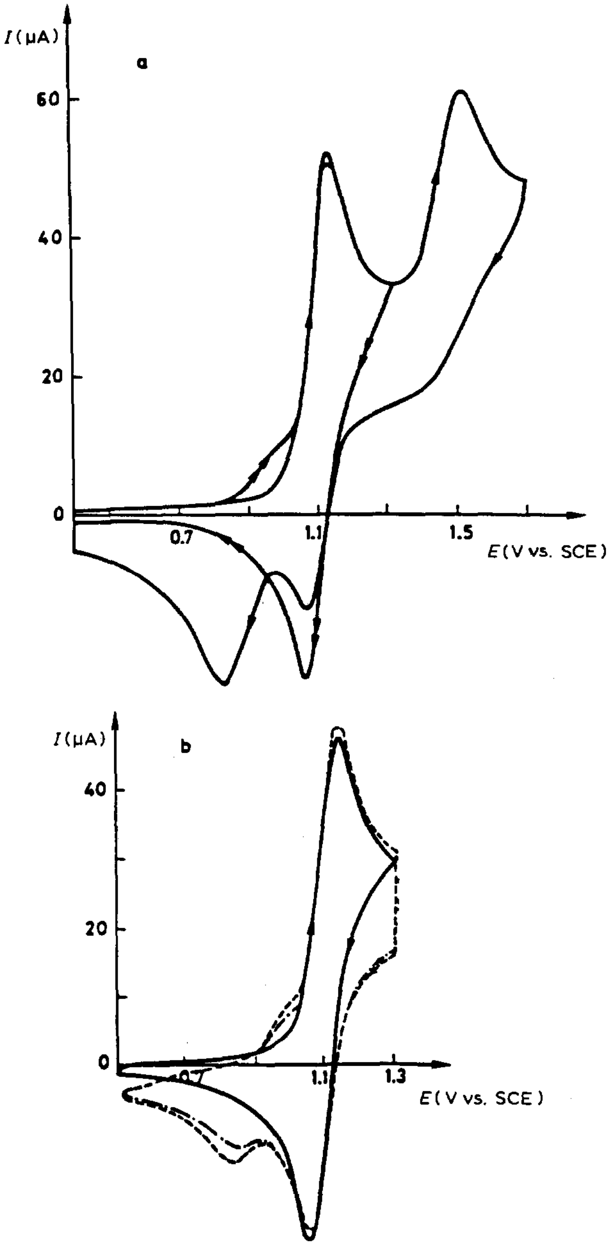

Fig. 3. Cyclic voltammograms of complex **1b** (1.2×10^{-3} mol dm^{-3}) in acetonitrile containing [Bu_4N][PF_6]. Pt electrode. Potential scan rate 0.10 V s^{-1}: (a) from 0.40 to 1.70 V; (b) from 0.50 to 1.30 V (———), from 1.30 to 0.50 V after holding the potential at 1.30 V for 30 s (·—·—·) and 60 s (— — —).

That there is kinetic control of the electrode process is revealed by the dependence of the current function $^3I_p^a v^{-1/2} c^{-1}$ on the scan rate (Fig. 4). As the value of the current function increases, approaching that for a two-electron process at the lower scan rates, disproportionation of the oxidised species seems likely. In the light

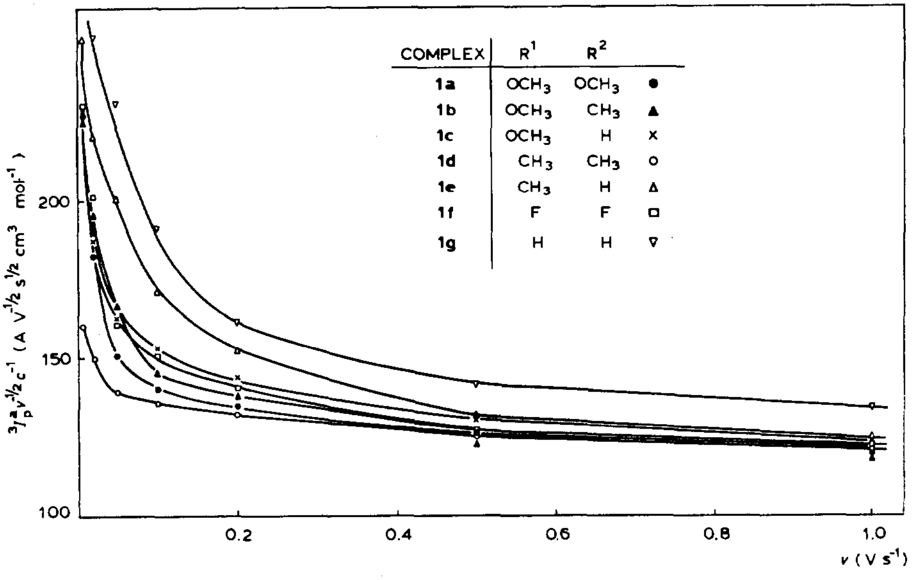

Fig. 4. Plots of the current function vs. potential scan rate for complexes **1a** to **1g**.

of these observations the following mechanism is proposed:

$$[\mathrm{MoCp_2(tri)}]^{+} \underset{+e}{\overset{-e}{\rightleftarrows}} [\mathrm{MoCp_2(tri)}]^{2+} \quad (\mathrm{tri} = \mathrm{dat, att, apt})$$

$$[\mathrm{MoCp_2(tri)}]^{2+} \overset{K_D}{\rightleftarrows} 1/2[\mathrm{MoCp_2(tri)}]^{+} + 1/2[\mathrm{MoCp_2(tri)}]^{3+}$$

$$[\mathrm{MoCp_2(tri)}]^{2+} \underset{+e}{\overset{-e}{\rightleftarrows}} [\mathrm{MoCp_2(tri)}]^{3+}$$

$$[\mathrm{MoCp_2(tri)}]^{3+} \rightarrow \mathrm{X}$$

Regeneration of the starting complex by the disproportionation accounts for the increasing values of the current functions at the lower scan rates. This is consistent with the formation of species X (responsible for wave 5) after the first oxidation. The disproportionation constants, K_D, presented in Table 2b, were calculated from the redox potential data. Although K_D values are small (in the order of 10^{-7}), the reaction proceeds at a reasonable rate owing to the fast reaction of its tricationic product.

Complex **1d** shows a reversible monoelectronic oxidation wave followed by an irreversible monoelectronic wave. However, the reduction wave 5 is never present. This, together with the almost negligible dependence of the current function on the scan rate, shows that the disproportionation reaction is not important for this complex.

The cyclic voltammograms for the complexes **1e**, **1f** and **1g** differ from those described previously, showing only one monoelectronic oxidation process together with the reduction peak at less positive potentials (Fig. 5a). As the potential scan rates increase the current ratios ${}^3I_p^c/{}^3I_p^a$ increase towards unity and the reduction peak 5 disappears (Fig. 5b). This means that the species obtained after oxidation of

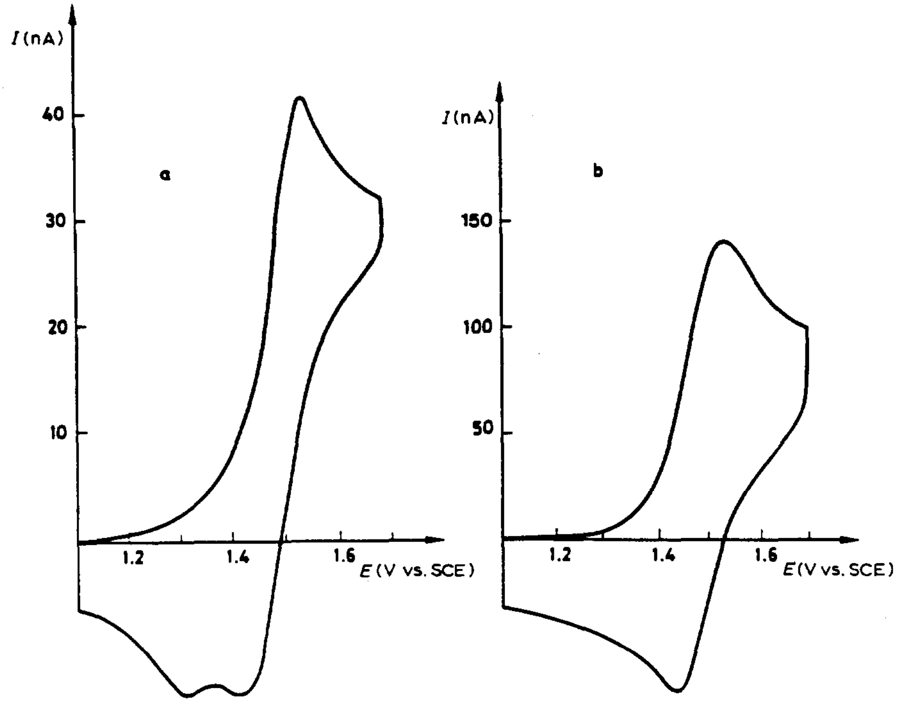

Fig. 5. Cyclic voltammograms of complex **1g** in acetonitrile at a microelectrode (Ø ~ 10 μm). Potential scan rate: (a) 100 V s^{-1}; (b) 800 V s^{-1}.

complexes **1e**, **1f** and **1g** are less stable than those obtained from the other complexes.

The lifetimes of the oxidised species presented in Table 2b were determined by Nicholson and Shain's method [10], the current ratios being calculated from an equation derived by Nicholson [11]. For complex **1g**, data were taken from cyclic voltammograms recorded at a platinum microelectrode [12], since reversible voltammograms could only be obtained at scan rates above 800 V s^{-1}.

These results show that the stability of the dications formed after the oxidation is dependent on the substituents R^1 and R^2, increasing with their electron donating ability. As expected from these observations the current functions for complexes **1e**, **1f** and **1g** have higher values than those for the other complexes. This is consistent with the disproportionation reaction referred to above.

To check whether the dication reacted with acetonitrile, whose bonding ability is well established [13], methylene dichloride was used as solvent. The constancy of the pattern obtained ruled out the hypothesis of a possible oxidatively induced reductive-elimination reaction, as was suggested for the complexes $[MoCp_2X_2]$ [14]. The possibility of interference by the supporting electrolyte (a potential source of the strong nucleophile, F^-) was also examined by replacing it with $[Bu_4N][ClO_4]$, but again the electrochemical behaviour was unchanged.

The reactions were also studied by constant potential electrolysis carried out in acetonitrile at potentials ca. 70 mV above ${}^3E_p^a$. For the complexes **1a**, **1b**, **1c**, **1e**, **1f** and **1g** (Figs. 6a and 6b) the current decay deviates from linearity as the electrolyses

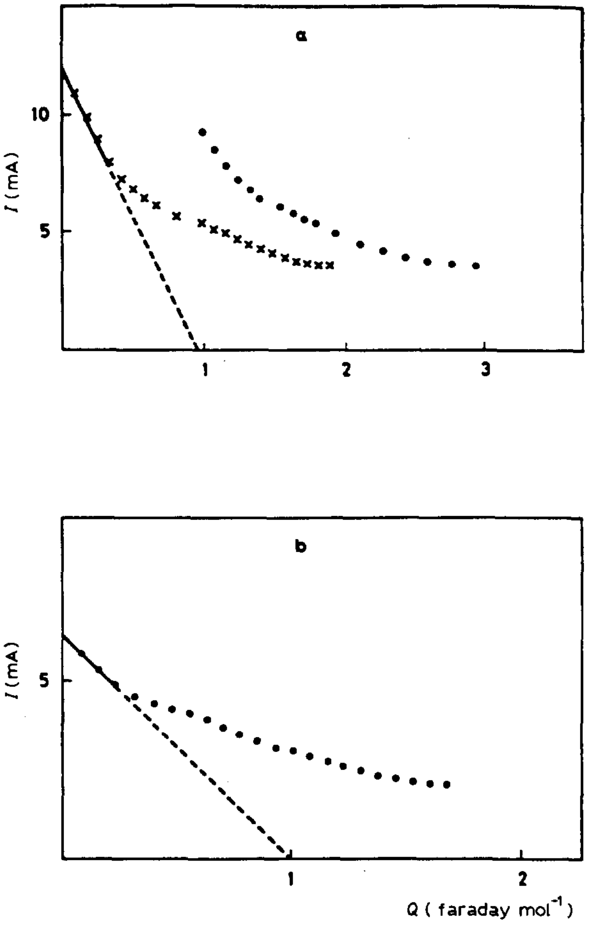

Fig. 6. Plots of the charge passed vs. cell current for the electrolysis of: (a) 50 μmol of complex **1a** in acetonitrile at +1.10 V (× × ×) and after interruption of the electrolysis when 4.82 C had passed (· · · · · ·); (b) 26 μmol of complex **1g** at 1.50 V.

proceed, a stationary current being obtained which is higher than the background current. The anolyte changes to dark red. A regular increase in the intensity of peak 3 towards a stationary value has also been observed in cyclic voltammograms run at successive instants after the electrolysis.

These observations are consistent with the occurrence of a disproportionation. The fact that the current value is higher than that expected for a linear decay reflects the contribution of the regeneration of the starting complex. The increase in peak intensity has a special meaning for complexes **1e**, **1f** and **1g**, for which no peak would be observed if the complexes were not regenerated by the chemical reaction. The electrolysis carried out with complex **1d** shows that the current is always proportional to the charge passed, 0.78 F mol^{-1} being consumed. This, together with a decrease in peak intensity observed in cyclic voltammograms run after the electrolysis, indicates that complex **1d** shows some instability.

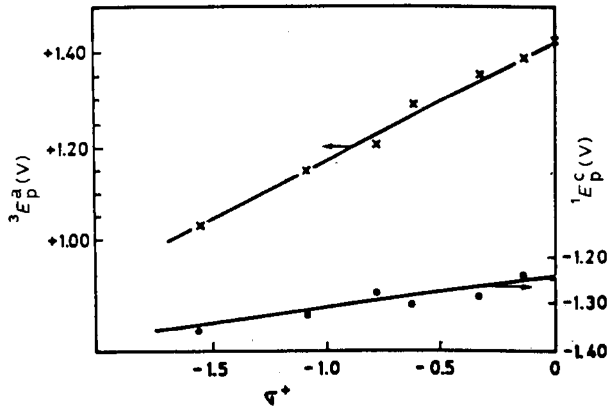

Fig. 7. Plots of oxidation potentials, $^{3}E_{p}^{a}$, and reduction potentials, $^{1}E_{p}^{c}$, against σ^{+} Hammett constants.

Correlations of the redox potentials with Hammett parameters

The potentials of the first oxidation peak, $^{3}E_{p}^{a}$, follow the expected trend as they become more positive when the substituents R^1 and R^2 are more electron withdrawing. This reflects the effect of the substituents on the energy of the redox orbital involved (HOMO). For the reduction peak potentials a shift was observed towards more negative potentials when the substituents become more electron donating. A good linear correlation was found for the oxidation potentials and the σ^{+} Hammett parameters [15], the correlation coefficient (r) being 0.994 (Fig. 7). A much poorer correlation was found with the σ Hammett parameters ($r = 0.940$). The same kind of pattern emerges from the analysis of the reduction potentials ($r = 0.987$). This suggests that mesomeric effects of the substituents play a major role.

From the slopes of the two straight lines it can be concluded that the effect of substituents is more pronounced on the oxidation potentials. Other authors observed a similar behaviour for some triazenido [3] and triazeneoxide [16] complexes and concluded that the oxidation occurs closer to the substituents. This means that the oxidation involves electrons on ligand based orbitals and the reduction is metal based. We believe that this conclusion is only valid when an inductive effect is present, in which case the number of bonds is of prime importance. When the influence is mesomeric no conclusive inferences can be drawn from this kind of observation. In order to clarify these aspects, ESR studies are in progress.

Experimental

Preparation of the complexes

The syntheses of the complexes were carried out under dinitrogen. Diaryltriazenes were prepared by reaction of the diazonium salts of p-$R^1C_6H_4NH_2$ with p-$R^2C_6H_4NH_2$ according to Vogel's method [17]. Complexes [$MoCpX_2$] (X = H, Cl, Br, I) were prepared as previously described [18,19].

Proton NMR spectra (of acetone-d_6 solutions) were recorded with a JEOL JNM 100 PFT instrument. Infrared spectra (of KBr pellets) were recorded on a Perkin–Elmer 457 instrument and calibrated with a polystyrene film. Conductivity data were determined using a Radiometer CDM3 conductimeter calibrated with a standard KCl solution.

Analyses for C, H and N were performed at the Centro de Química Estrutural, Lisbon.

Bis(η-cyclopentadienyl)(1,3-di-p-anisyltriazenido)molybdenum hexafluorophosphate (1a)

Method 1. A mixture of [$MoCp_2Br_2$] (0.38 g, ca. 1 mmol), 1,3-di-*p*-anisyltriazene (0.40 g, ca. 1.5 mmol), and triethylamine (1 ml) in ethanol was refluxed for 1 h. Addition of [NH_4][PF_6] to the filtered red solution, followed by partial evaporation of the solvent yielded a red precipitate. This was washed with water, dried, and recrystallised from acetone/petroleum ether as red crystals (yield 75%).

Method 2. [$MoCp_2H_2$] (0.23 g, ca. 1 mmol), 1,3-di-*p*-anisyltriazene (0.40 g, ca. 1.5 mmol) were treated in the same way as in method 1 (yield 75%).

The other complexes were prepared by the same method by use of the appropriate 1,3-diaryltriazene.

Electrochemical measurements

Acetonitrile (Merck) was purified by a published method [20], methylene dichloride (Merck) was distilled from CaH_2; both were stored over activated alumina. Tetrabutylammonium perchlorate (Fluka) was dried over P_2O_5. Tetrabutylammonium hexafluorophosphate was prepared from tetrabutylammonium bromide (Merck) and ammonium hexafluorophosphate (Merck) in ethanol, and was recrystallised from acetone/ethanol and dried under vacuum.

The electrochemical studies were performed with a PAR 174 Polarographic Analyser and a PAR 175 Universal Programmer linked to a Philips PM 8041 X-Y recorder. For scan rates above 0.50 V s^{-1} a digital Nicolet Explorer 2090 II oscilloscope was used. Cyclic voltammetry was carried out under dinitrogen with a three electrode cell. The working electrode was a platinum wire, the auxiliary electrode was a platinum helix and potentials were referred to a saturated calomel electrode.

The microelectrode experiments were carried out with a two electrode cell, where the platinum electrode had a diameter of 10 μm and the reference electrode, also used as the auxiliary electrode, was a mercury pool.

Constant potential electrolyses (30 to 60 μmol of complex in each experiment) were taken with an H-type three electrode, three compartment cell, with an electrolyte volume of 20 cm^3. Platinum gauze working and auxiliary electrodes of 1 cm^2 area were used. The charge was monitored with an integrator.

References

1 R. Rossi, A. Duatti, L. Magnon and L. Toniolo, Inorg. Chim. Acta, 48 (1981) 243 and references therein.

2 C.J. Pickett in D. Pletcher (Ed.), Electrochemistry (Specialist Periodical Reports) London, vol. 8 (1983) and vol. 9 (1984).

3 J.G.M. Van der Linden, A.H. Dix and E. Pfeiffer, Inorg. Chim. Acta, 39 (1980) 271.

4 W.J. Geary, Coord. Chem. Rev., 7 (1973) 81.

5 J.C. Kotz, W. Wining, W. Coco, A.R. Dias and M.H. Garcia, Organometallics, 2 (1983) 68.

6 (a) Y. Mugnier, C. Moise and E. Laviron, J. Organomet. Chem., 204, 61 (1981); (b) ibid., 6 (1982) 197; (c) A. Fakhr, Y. Mugnier, R. Broussier, B. Gautherion and E. Laviron, J. Organomet. Chem., 255 (1983) C8.
7 G. Zotti, S. Zechini and G. Pilloni, J. Organomet. Chem., 246 (1983) 61.
8 W.A. Fordyce, K.H. Pool and G.A. Crosby, Inorg. Chem., 21 (1982) 1027.
9 E. Maerlik, J. Hanzlik, A. Camus, G. Mestroni and G. Zassinovich, J. Organomet. Chem., 112 (1977) 95.
10 R.S. Nicholson and I. Shain, Anal. Chem., 36 (1964) 760.
11 R.S. Nicholson, Anal. Chem., 38 (1966) 1406.
12 M.I. Montenegro, Portugaliae Electroquimica Acta, 3 (1985) 165.
13 M.J. Calhorda, M.A.A.F. de C.T. Carrondo, A.R. Dias, A.M.T. Domingos, M.T.L.S. Duarte, M.H. Garcia and C.C. Romão, J. Organomet. Chem., 320 (1987) 63.
14 J.C. Kotz, private communication.
15 R.A.I. Jones, Physical Mechanistic Organic Chemistry, Cambridge Univ. Press, 1979.
16 R.N. Muckerjee, O.A. Rajan and A. Chakravorty, Inorg. Chem., 21 (1982) 78.
17 A. Vogel, Practical Organic Chemistry, Longmans, London, 1978, p. 720.
18 M.L.H. Green and P.J. Knowles, J. Chem. Soc., Perkin Trans., 7 (1973) 989.
19 R.L. Cooper and M.L.H. Green, J. Chem. Soc. A, (1967) 1155.
20 C.K. Mann, in A.J. Baird (Ed.), Electroanalytical Chemistry, Marcel Dekker, New York, 1969, Vol. 3, p. 58.